

NASA Technical Memorandum **104190**

104190 /
p 23

APPLICATION OF PROGRAM LAURA TO PERFECT GAS SHOCK TUBE FLOWS -- A PARAMETRIC STUDY

K. F. Mitterer

R. A. Mitcheltree

P. A. Gnoffo

(NASA-TM-104190) APPLICATION OF PROGRAM
LAURA TO PERFECT GAS SHOCK TUBE FLOWS: A
PARAMETRIC STUDY (NASA) 23 0 CSCL 200

NO2-17002

and 175

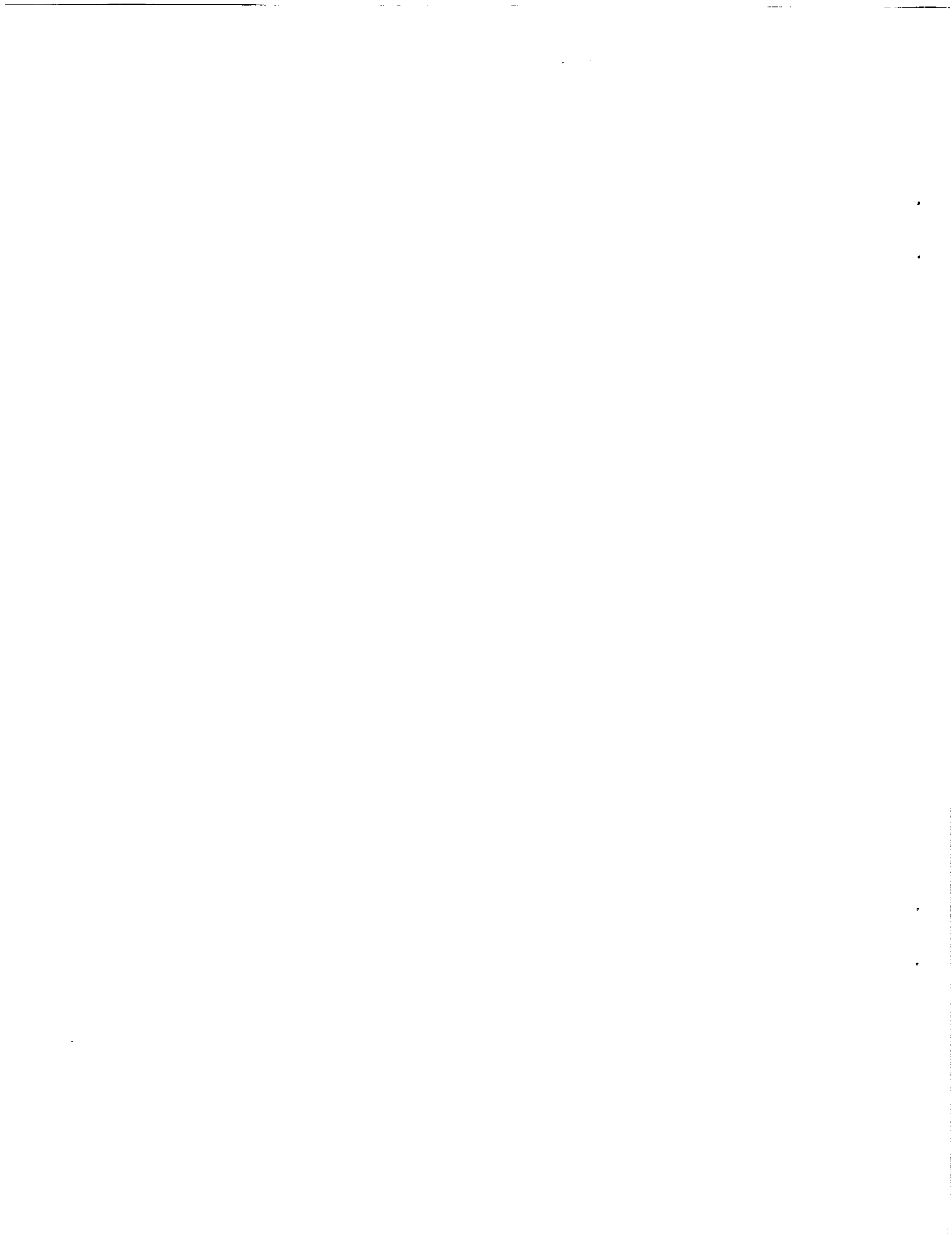
5/7/84 0052237

January 1992

NASA

National Aeronautics and
Space Administration

Langley Research Center
Hampton, Virginia 23665



APPLICATION OF PROGRAM LAURA TO PERFECT GAS SHOCK TUBE FLOWS A Parametric Study

K. F. Mitterer* and R. A. Mitcheltree † and P. A. Gnoffo ‡
NASA Langley Research Center, Hampton, Virginia

Introduction

The Langley Aerothermodynamic Upwind Relaxation Algorithm (LAURA) was originally developed by Gnoffo¹ to solve steady-flow problems. The desire to validate the algorithm with shock tube experimental data² has motivated the development of a time-accurate version of the LAURA code. Using the LAURA scheme in this manner is not the optimal approach to the solution of unsteady flow problems, but the code is easily modified to produce time-accurate results.

The objective of this work is to develop and test the time-accurate version of LAURA. The algorithm's modifications are discussed in the next section. Testing the solution accuracy of LAURA is accomplished by comparing the computational results with an exact solution. For this purpose the present study is solely concerned with inviscid, perfect-gas shock tube flow. Real gas effects will be examined in subsequent studies. The approach to analyzing the overall solution accuracy of LAURA is discussed in the section entitled *Parameters of the Study*.

Time-Accurate Relaxation Algorithm

The governing equation for inviscid flow of a perfect gas may be written

$$\iiint \frac{\partial \mathbf{q}}{\partial t} d\Omega + \iint \bar{\mathbf{f}} \cdot \bar{\mathbf{n}} d\sigma = 0 \quad (1)$$

*Co-op Student, Aerothermodynamics Branch, Space Systems Division, NASA Langley Research Center

†Aerospace Engineer, Aerothermodynamics Branch, Space Systems Division, NASA Langley Research Center

‡Senior Researcher, Aerothermodynamics Branch, Space Systems Division, NASA Langley Research Center

In Eq. 1 the first term describes the time rate of change of conserved quantity \mathbf{q} in the control volume Ω and the second term describes the convective flux $\vec{\mathbf{f}}$ through the cell walls; $\vec{\mathbf{n}}$ is the unit vector normal to the cell walls and σ is the cell wall area. The finite-volume formulation of Eq. 1 is given by

$$\left[\frac{\delta \mathbf{q}}{\delta t} \Omega\right]_L + \sum_{l=i,j,k} [\vec{\mathbf{f}}_{l+1} \cdot \vec{\mathbf{n}}_{l+1} \sigma_{l+1} - \vec{\mathbf{f}}_l \cdot \vec{\mathbf{n}}_l \sigma_l] = 0 \quad (2)$$

Note in Eq. 2 that uppercase integer variables L denote computational coordinates at cell centers, and lowercase integer variables l denote cell faces. We define $\mathbf{g}_l = \vec{\mathbf{f}}_l \cdot \vec{\mathbf{n}}_l$ so that Eq. 2 becomes

$$\left[\frac{\delta \mathbf{q}}{\delta t} \Omega\right]_L + \sum_{l=i,j,k} [\mathbf{g}_{l+1} \sigma_{l+1} - \mathbf{g}_l \sigma_l] = 0 \quad (3)$$

where

$$\mathbf{q} = \begin{bmatrix} \rho \\ \rho u \\ \rho v \\ \rho w \\ \rho E \end{bmatrix} \quad (4)$$

$$\mathbf{g} = \begin{bmatrix} \rho U \\ \rho U u + p n_x \\ \rho U v + p n_y \\ \rho U w + p n_z \\ \rho U H \end{bmatrix} \quad (5)$$

In Eqs. 4 and 5 ρ represents density, u , v , and w are the scalar components of velocity, E is the total energy per unit mass, U is the normal component of velocity through the cell wall, P is the pressure, and H represents the total enthalpy per unit mass.

The governing relaxation equation in the LAURA¹ code for inviscid, steady flow is defined by

$$\mathbf{q}_L^{n+1} = \mathbf{q}_L^n + \mathbf{M}_L^{-1} \mathbf{r}_L \quad (6)$$

where \mathbf{M}_L is the point-implicit Jacobian given by

$$\mathbf{M}_L = \frac{r f_{INV}}{2} \sum_{l=i,j,k} [|\mathbf{A}_{l+1}| \sigma_{l+1} + |\mathbf{A}_l| \sigma_l]^n \quad (7)$$

and \mathbf{r} is the right-hand-side solution (residual) vector given by

$$\mathbf{r}_L = - \sum_{l=i,j,k} [\mathbf{g}_{l+1} \sigma_{l+1} - \mathbf{g}_l \sigma_l]^n \quad (8)$$

Spatial differencing of the residual vector can be either first or second order accurate. In Eq. 7 r_{fINV} represents the inviscid relaxation factor. The matrix $|A_l|$ is the Roe's averaged³ Jacobian of \mathbf{g} with respect to \mathbf{q} at cell wall l with absolute, limited eigenvalues as described in Ref. 1.

We employ M local relaxation steps before advancing a time step Δt to obtain first order accuracy in time in the following manner.

$$\mathbf{q}_L^{n,m+1} = \mathbf{q}_L^{n,m} + \mathbf{M}_L^{-1} \mathbf{r}_L \quad (9)$$

$$\mathbf{M}_L = \frac{r_{fINV}}{2} \sum_{l=i,j,k} [|A_{l+1}| \sigma_{l+1} + |A_l| \sigma_l]^{n,1} + \frac{\Omega_L}{\Delta t} \mathbf{I} \quad (10)$$

and

$$\mathbf{r}_L = - \sum_{l=i,j,k} [\mathbf{g}_{l+1} \sigma_{l+1} - \mathbf{g}_l \sigma_l]^{n,m} - \frac{\mathbf{q}_L^{n,m} - \mathbf{q}_L^{n,1}}{\Delta t} \Omega_L \quad (11)$$

In Eq. 10 \mathbf{I} represents the identity matrix. After M local iterations, the solution is advanced to time step $n + 1$ by setting

$$\mathbf{q}_L^{n+1,1} = \mathbf{q}_L^{n,M} \quad (12)$$

The number of local iterations M should be large enough such that the residual error defined by Eq. 11 above is smaller than $O(\Delta t)$. Extensions of this method to viscous, nonequilibrium flows are trivial, but as yet untested.

Parameters of the Study

The parametric study is conducted to define the uncertainty and computational cost associated with applying LAURA to unsteady flow problems. The parameters examined include Courant number, grid resolution, relaxation sweeps, and the inviscid relaxation factor.

For the simple shock tube, Courant number defines the number of cells the shock wave propagates every time step.

$$cn = \frac{\lambda \delta t}{\delta x} \quad (13)$$

where, λ is the velocity of the shock wave, δt is the time step, and δx is the grid spacing. If δx is constant then Courant number varies with δt . The effect of the time step on a solution may

be examined by varying the Courant number. Decreasing the time step improves accuracy at the price of additional computational cost.

The grid spacing is related to the number of cells in the grid.

$$\delta x = \frac{\text{grid extent}}{\text{cells}} \quad (14)$$

Increasing the number of grid cells improves the grid resolution and solution accuracy. This improved accuracy carries with it additional computational cost.

The number of relaxation sweeps is the number of iterations performed to “relax” the solution ahead one time step. With a sufficient number of relaxation sweeps the solution converges to time-accuracy. There is a direct trade-off between relaxation sweeps and computational cost. This trade-off prompts an investigation into the minimum number of relaxation sweeps required to obtain a time-accurate converged solution.

The inviscid relaxation factor is the only parameter to be studied with no associated trade-off in computational cost. The rf_{INV} was initially implemented in the algorithm to increase the stability of the scheme. Two values of rf_{INV} are examined in this study: $rf_{INV}=1.5$ and $rf_{INV} = 2.0$. Indirectly, this factor controls the speed with which a solution converges.

The parametric study is conducted to analyze the capabilities of the time-accurate LAURA code in predicting unsteady flow solutions. The four coupled parameters are isolated to examine the contribution of each to the overall accuracy of a LAURA solution. The study examines discrete values for each of the parameters. The results suggest preferred values for each parameter to efficiently achieve time-accurate solutions. These suggested values for the parameters, while not completely optimized, are selected by examining trends in the parametric study.

Test Case and Computational Mesh

The initial conditions of the simple shock tube test case are taken from Ref. 4. The low pressure side of the diaphragm is initialized with standard atmospheric conditions at sea level. The pressure ratio across the diaphragm is 10. The density ratio is 8. Both sides have zero initial velocity. The shock tube test case assumes inviscid, perfect gas ($\gamma = 1.4$).

A one-dimensional computational grid extending from -0.5 m to 0.5 m with the diaphragm at 0.0 m is used in the calculations. Grids of 200, 400, 800, 1600 and 3200 cells are examined. All solutions are computed at time equals 4.5×10^{-4} sec.

Results

Results shown from the parametric study systematically progress toward obtaining the best time-accurate LAURA solution by isolating the individual parameters. The progression of the results examines the contributions of relaxation sweeps, Courant number, inviscid relaxation factor, and grid spacing toward a time-accurate LAURA solution. The investigation begins with a comparison between first and second order accurate spatial differencing.

Figure 1 displays the nondimensionalized density distribution, as calculated using first and second order accurate spatial differencing, compared to the exact solution. The Courant number for these computational solutions is 0.1. Twenty relaxation sweeps are taken for each time step over a computational grid of 200 cells. The second order accurate solution is computed in approximately 2600 seconds on a Sun SPARCstation. Figures 2 and 3 show the pressure and velocity distributions for the comparison in Fig. 1. The additional accuracy obtained from second order differencing legitimizes its sole use in the remaining results of this study. Trends appearing in the velocity and pressure distributions are evident in the density distribution, notably, the dissipation existing across the shock and the expansion head. Thus, the results of the parametric study are discussed with regard to the density distributions of the solutions.

The effects of the number of relaxation sweeps can be isolated by holding the Courant number constant. Figure 4 displays the solutions for a constant Courant number of 2 and relaxation sweeps of 10, 20, and 200. In this plot the number of relaxation sweeps is seen to affect the time-accuracy of a solution. Figure 5 examines the relaxation sweeps effect for a Courant number of 1. The only noticeable difference between 10 and 200 relaxation sweeps occurs across the shock; the 10 and 20 relaxation sweeps solutions overlap. Figure 6 shows that for $cn=0.5$, 10 relaxation sweeps is enough to obtain a time-accurate solution.

The two components of overall solution accuracy are time-accuracy and quality. Time-accuracy

is revealed by the calculated location of the shock, contact surface, and expansion wave compared to the locations predicted by the analytic solution. The quality is the degree of dissipation of the solution. Examining Figs. 4, 5, and 6 reveals that the number of relaxation sweeps affects the time-accuracy of a solution and the Courant number affects the dissipation of a solution. In Fig. 7 it is apparent that 5 relaxation sweeps is enough to obtain a converged solution for $cn=0.1$. Comparing the dissipation in Fig. 7 with that of Figs. 4, 5, and 6, it is clear that decreasing the Courant number produces solutions of less dissipation. Decreasing the Courant number any more than 0.1, however, increases the computational cost for a negligible gain in accuracy.

If time-accuracy can be achieved for less than 5 relaxation sweeps by varying the inviscid relaxation factor, computational cost will be cut. Figures 8 and 9 display the effects of rf_{INV} on the solution accuracy. In Fig. 8 the rf_{INV} is lowered from 2.0 to 1.5 for the 2 relaxation sweeps case. It appears that lowering the rf_{INV} to 1.5 helps converge a solution that is not time-accurate. Figure 9 shows instability at the expansion tail caused by $rf_{INV}=1.5$ for a Courant number of 2. This instability might be removed by updating the Jacobian of Eq. 7 more often than once per time step. The study also revealed, however, that a solution with $rf_{INV}=2.0$ may actually converge to time-accuracy before a solution with $rf_{INV}=1.5$ regardless of Courant number.

The results thus far have used a computational grid of 200 cells. The highest quality LAURA solution is the case with $cn=0.1$, $rf_{INV}=2.0$, and 5 relaxation sweeps. The remainder of the study will examine the effect of increasing the grid resolution.

Figure 10 compares the 200, 400, and 800 grid cells solutions. It is apparent that increasing the grid resolution improves the quality of the solution. The price of this increased quality is computational cost. The solution for 800 cells is computed in 41000 sec. Figure 11 reveals that increasing the number of grid cells to 3200 produces a better approximation of the exact solution. At this scale there is little noticeable difference between the 800 grid cells solution and the 3200 grid cells solution. Figure 12 displays in detail the shock and contact surface shown in Fig. 11.

Increasing the number of grid cells significantly adds to the computational cost of the solutions. At increased grid resolution, it would be advantageous if an accurate solution could be found for less

than 5 relaxation sweeps. Figure 13 shows that across the shock a noticeable difference exists for the 2 and 5 relaxation sweeps solutions. This result points out that while increasing the grid resolution significantly decreases the dissipation there is a less pronounced effect on the time-accuracy of a LAURA solution.

Conclusions

This parametric study of a time-accurate version of LAURA applied to inviscid, perfect-gas shock tube flow is an investigation into the trade-offs between overall solution accuracy and computational cost. The results of the study lead to some interesting conclusions concerning the effect of the parameters, the best LAURA solution, and computational cost of the solutions.

The four parameters examined are Courant number, relaxation sweeps, inviscid relaxation factor, and grid spacing. The parametric study indicates that these coupled parameters have, in fact, isolated effects on the solutions. The Courant number and grid spacing significantly affect the dissipation of the solution, while the number of relaxation sweeps and the inviscid relaxation factor affect the time-accuracy of the solution. As would be expected, second order accurate spatial differencing results in higher resolution quality than first order accurate spatial differencing.

Finding the best time-accurate LAURA solution was a primary goal of this study. The best solution is defined as the solution with the highest degree of accuracy for the least computational cost. For a grid of 200 cells, the best solution is $cn=0.1$ with 5 relaxation sweeps. The results of the study indicate that LAURA is capable of producing extremely accurate solutions by increasing the number of grid cells. This study was limited to the maximum of 3200 grid cells in consideration of excessive computational time. It appears that by increasing the number of grid cells the quality of the solution will continue to improve.

The price of highly resolved solutions is considerable computational cost. The solution of the $cn=0.1$, 5 relaxation sweeps, and 200 grid cells case is computed in about 43 minutes. Increasing the grid to 800 cells, while holding Courant number and number of relaxation sweeps constant, increases the computational time by a factor of 16.

References

¹Gnoffo, P. A., Gupta, R. N., and Shinn, J. L., "Conservation Equations and Physical Models for Hypersonic Air Flows in Thermal and Chemical Nonequilibrium," NASA Technical Paper 2867, February, 1989.

²Sharma, S. P., Gillespie, W. D., and Meyer, S. A., "Shock Front Radiation Measurements in Air," AIAA Paper AIAA-91-0573, January, 1991.

³Roe, P. L., "Approximate Riemann Solvers, Parameter Vectors, and Difference Schemes," J. of Comput. Phys., Vol. 43, no. 2, October, 1981, pp. 357-372.

⁴Sod, G. A., "A Survey of Several Finite Difference Methods for Systems of Nonlinear Hyperbolic Conservation Laws," J. of Comput. Phys., Vol. 27, no. 1, April, 1978, pp. 1-31.

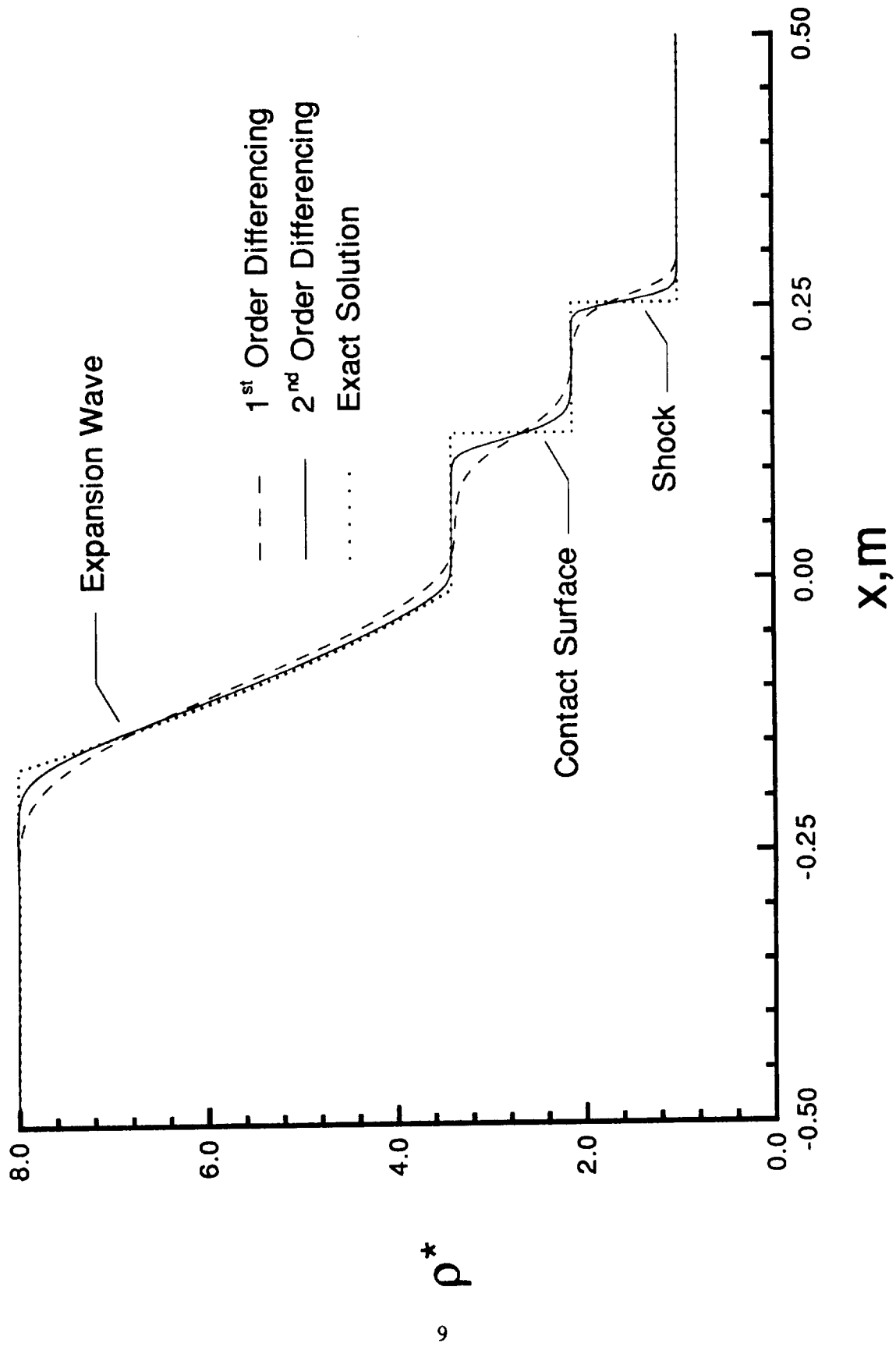


Figure 1. Effect of spatial-differencing accuracy on the nondimensional density distribution.

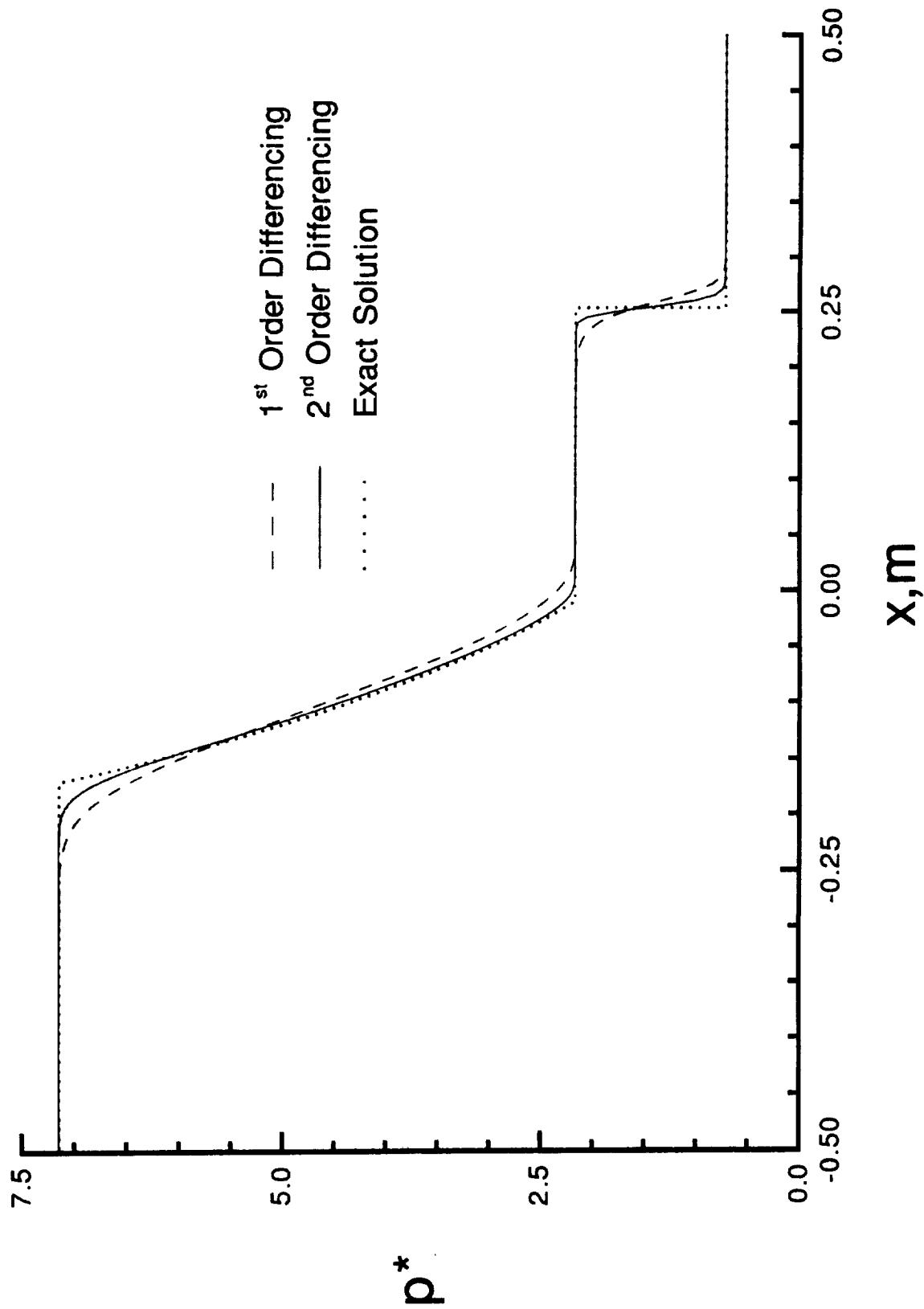


Figure 2. Effect of spatial-differencing accuracy on the nondimensional pressure distribution.

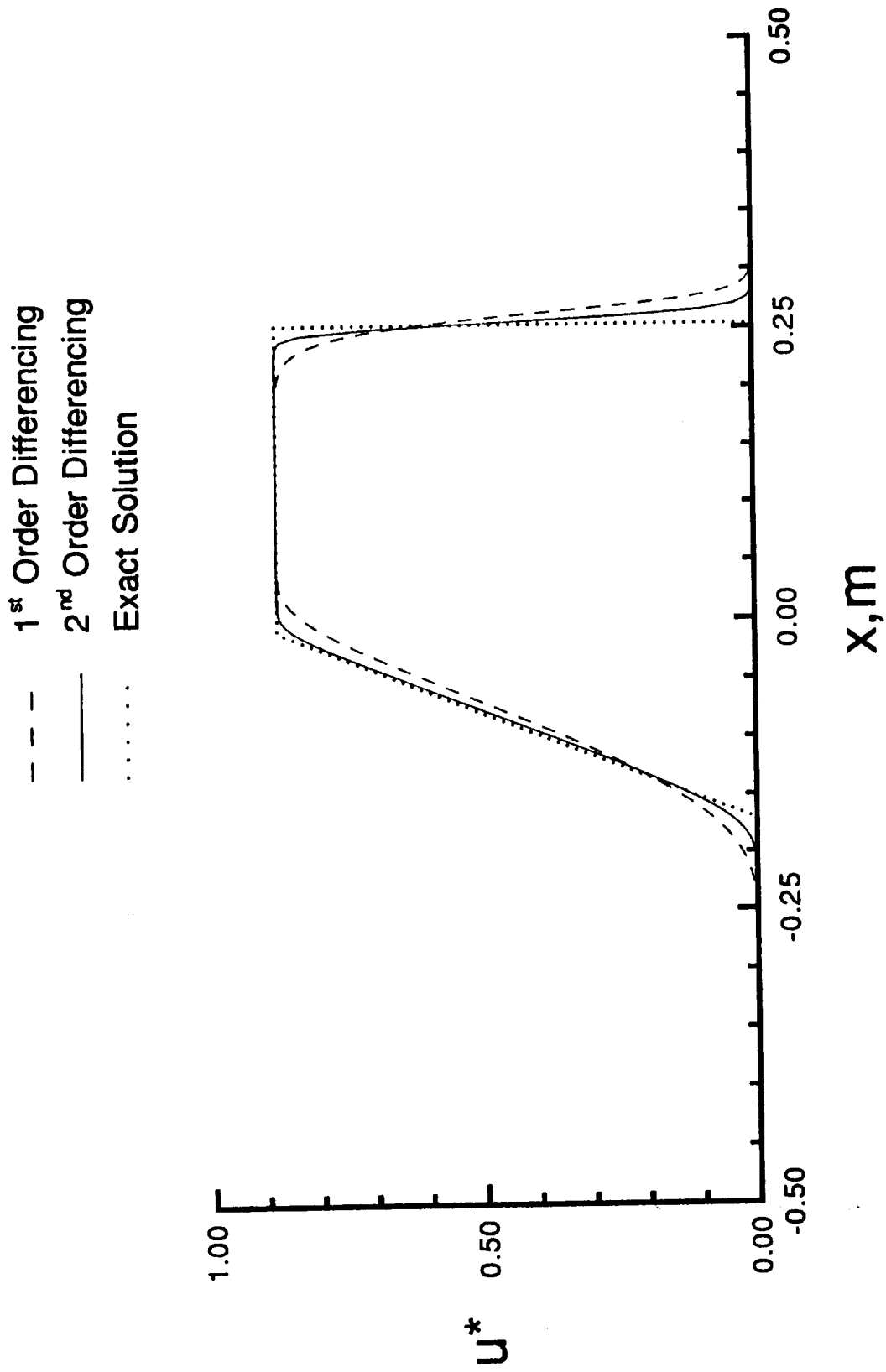


Figure 3. Effect of spatial-differencing accuracy on the nondimensional velocity distribution.

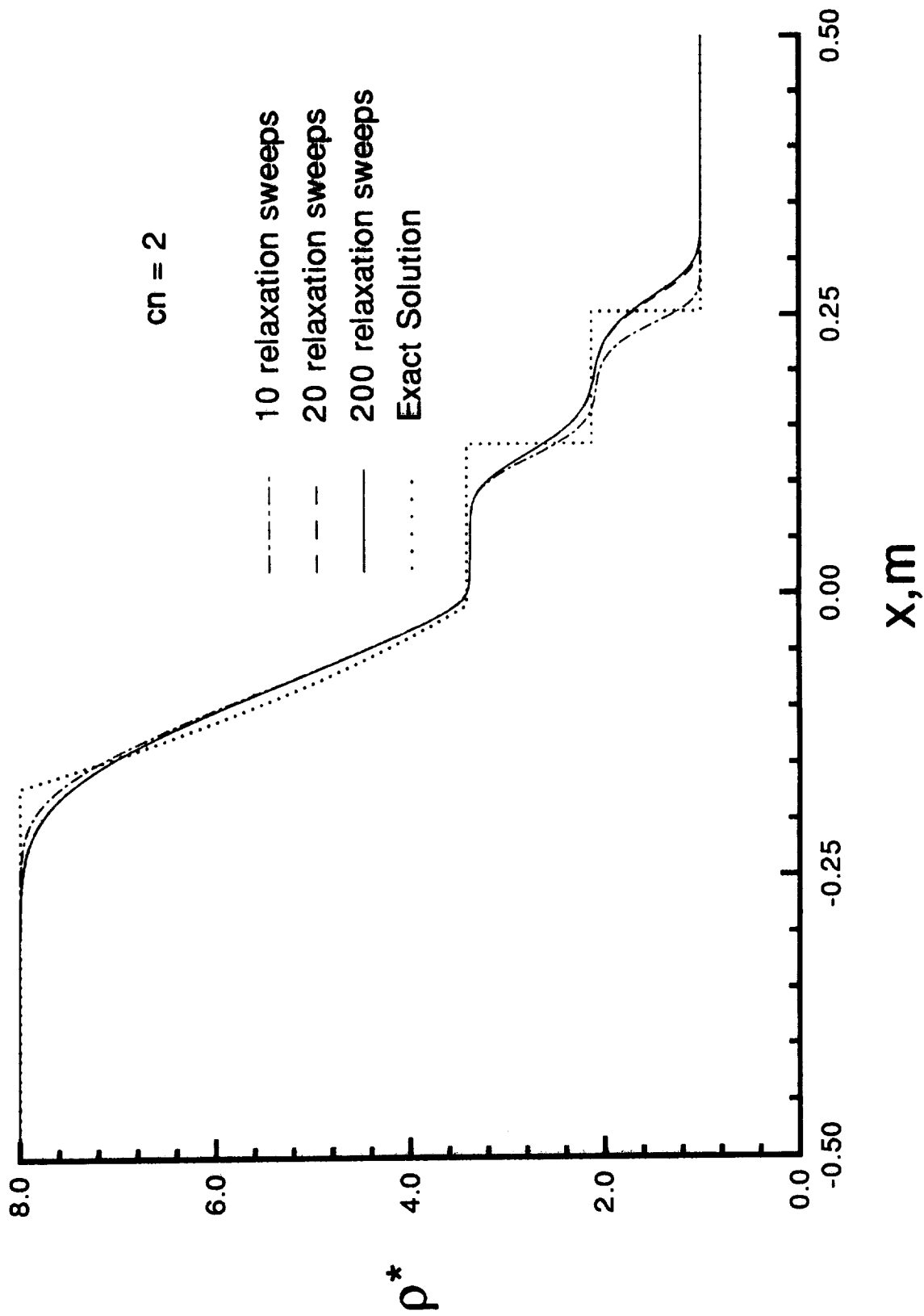


Figure 4. Effect of relaxation sweeps on the nondimensional density distribution for $cn=2$.

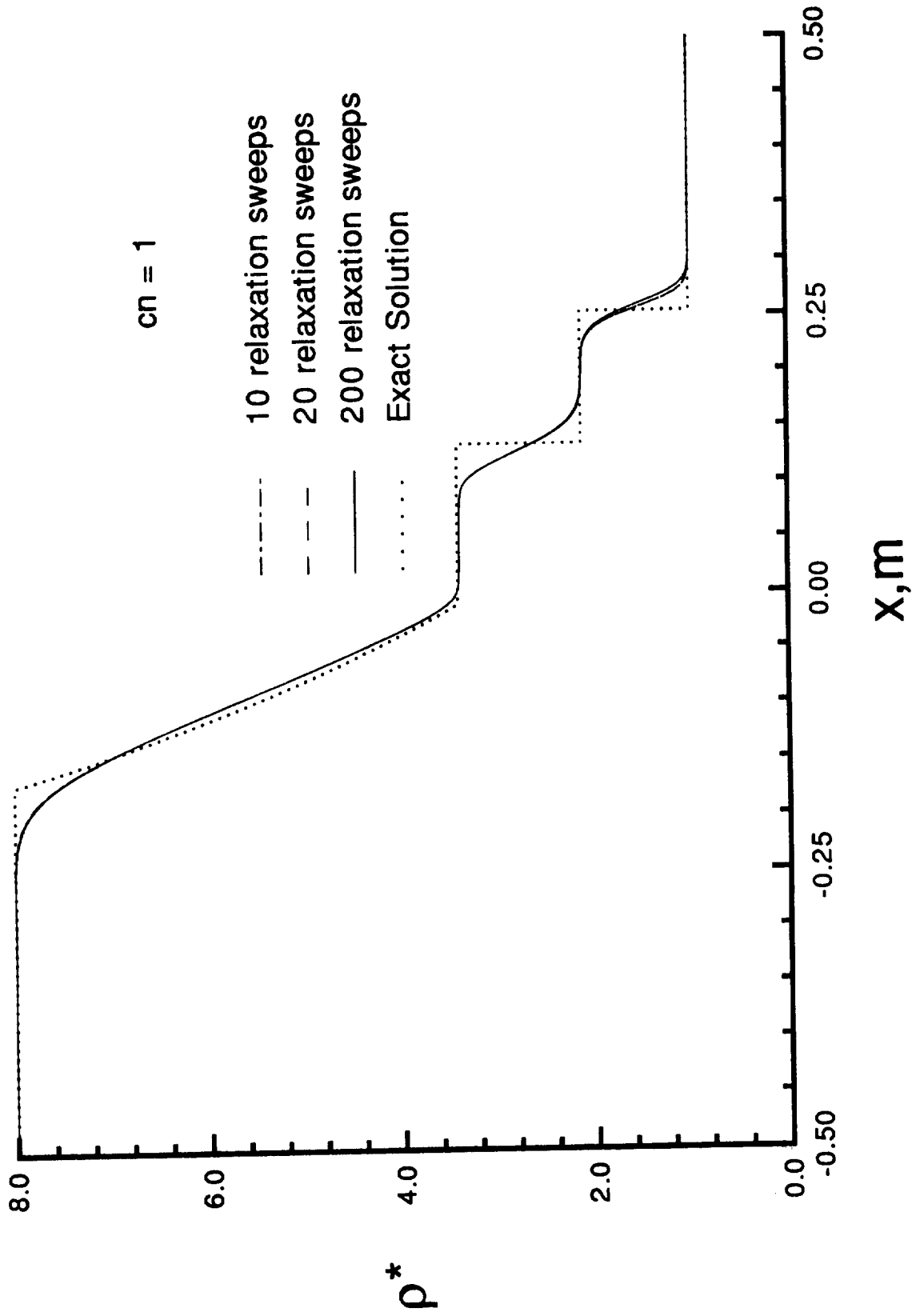


Figure 5. Effect of relaxation sweeps on the nondimensional density distribution for $cn=1$.

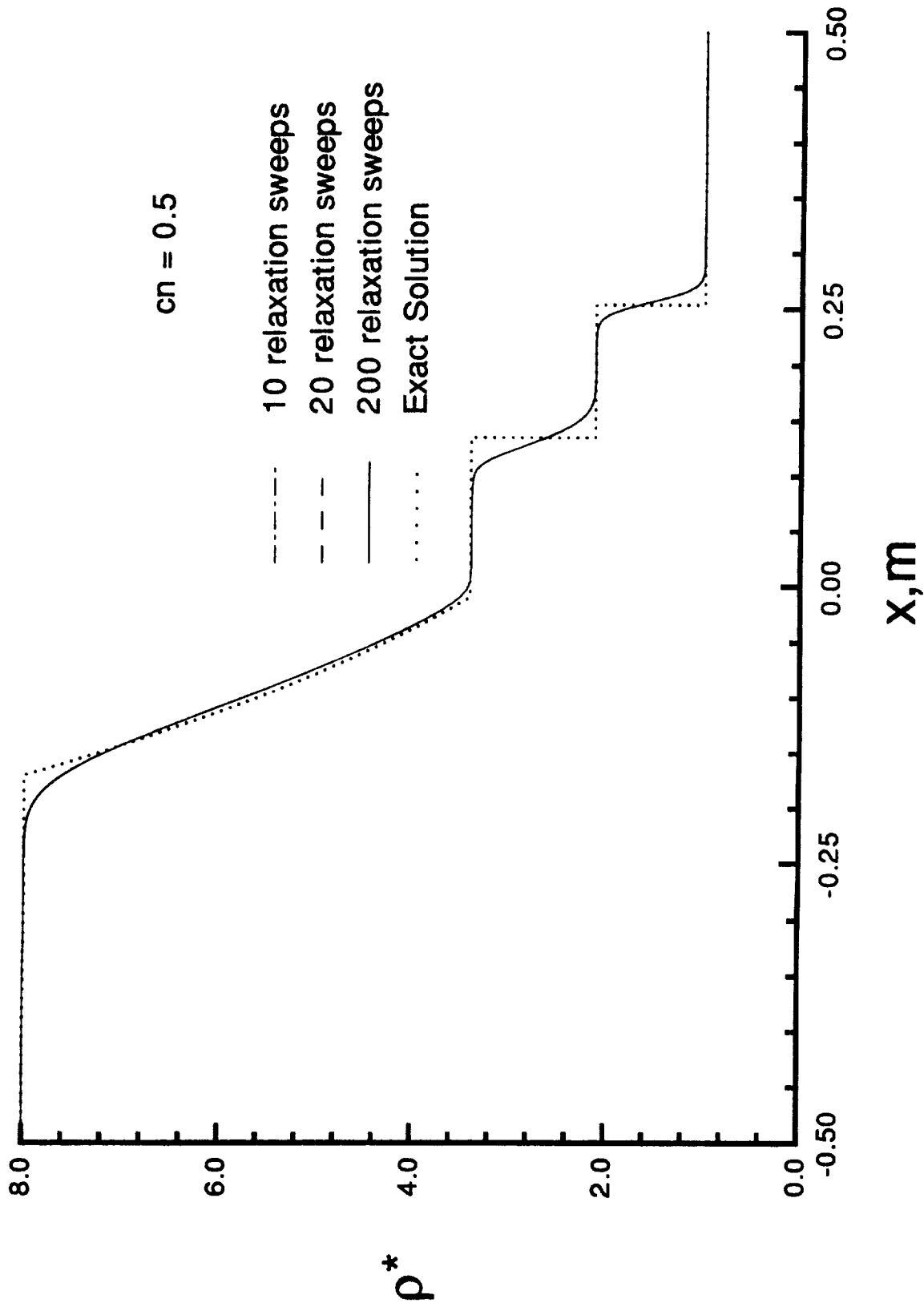


Figure 6. Effect of relaxation sweeps on the nondimensional density distribution for $cn=0.5$.

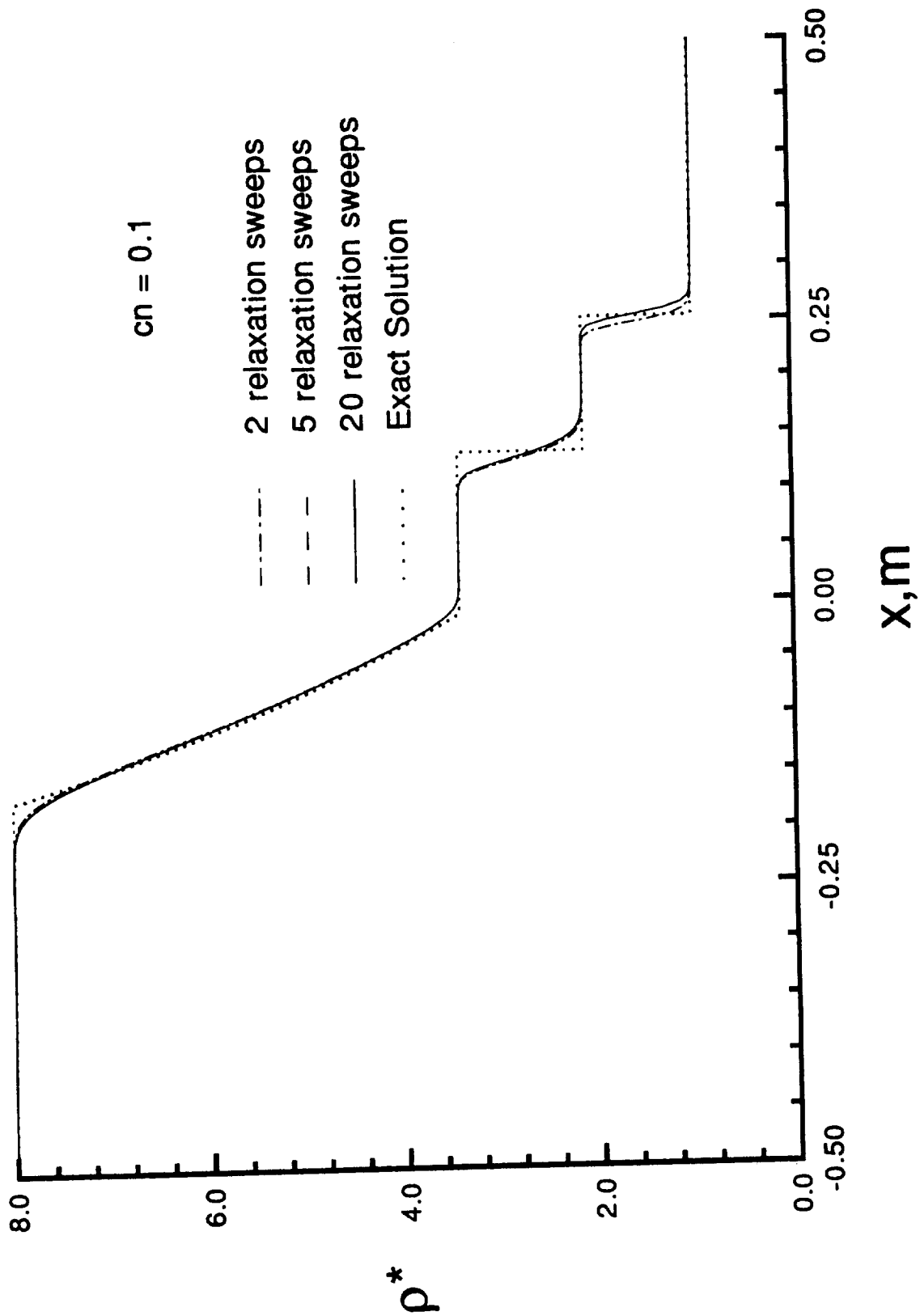


Figure 7. Effect of relaxation sweeps on the nondimensional density distribution for $cn=0.1$.

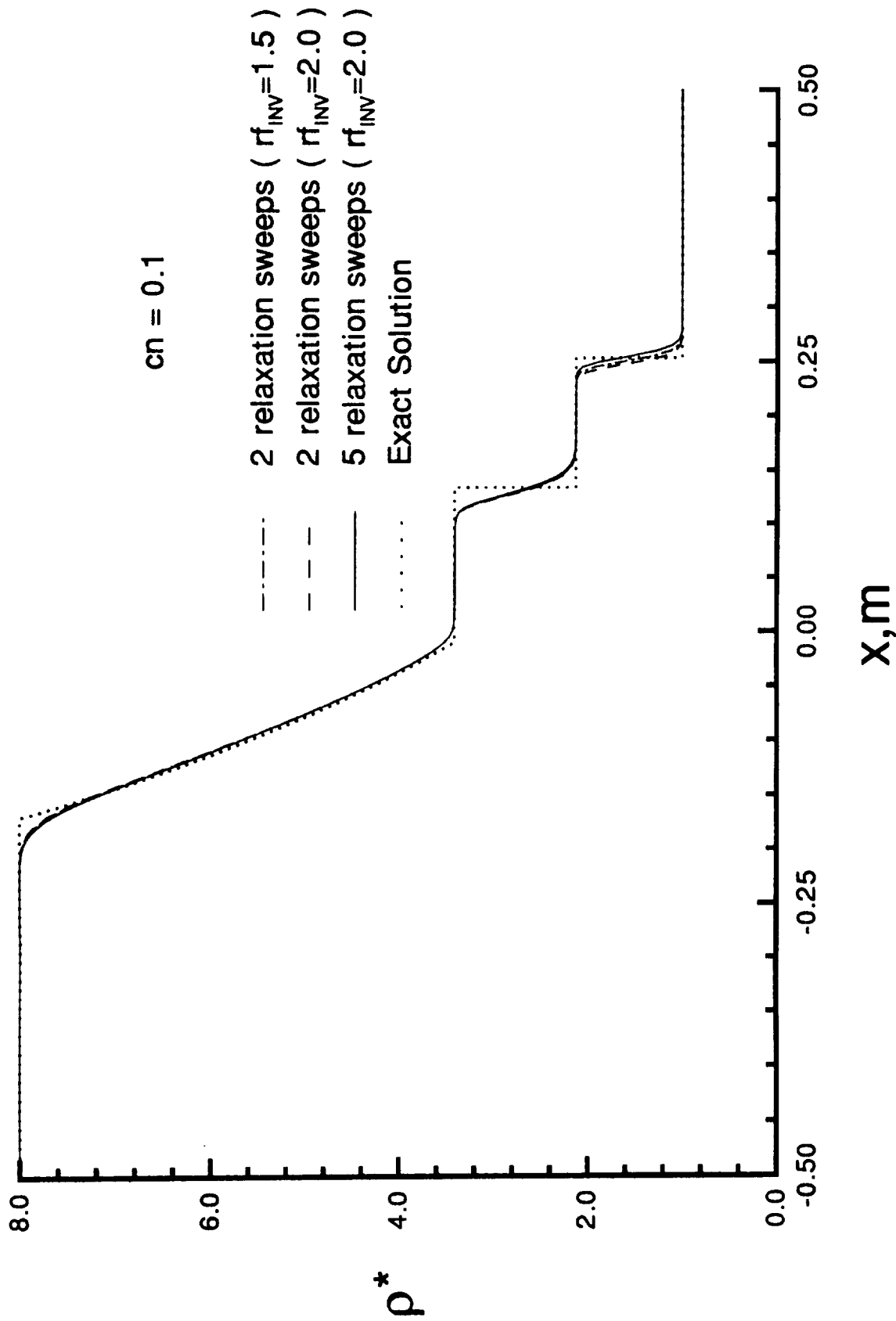


Figure 8. Effect of the inviscid relaxation factor on the nondimensional density distribution for $cn=0.1$.

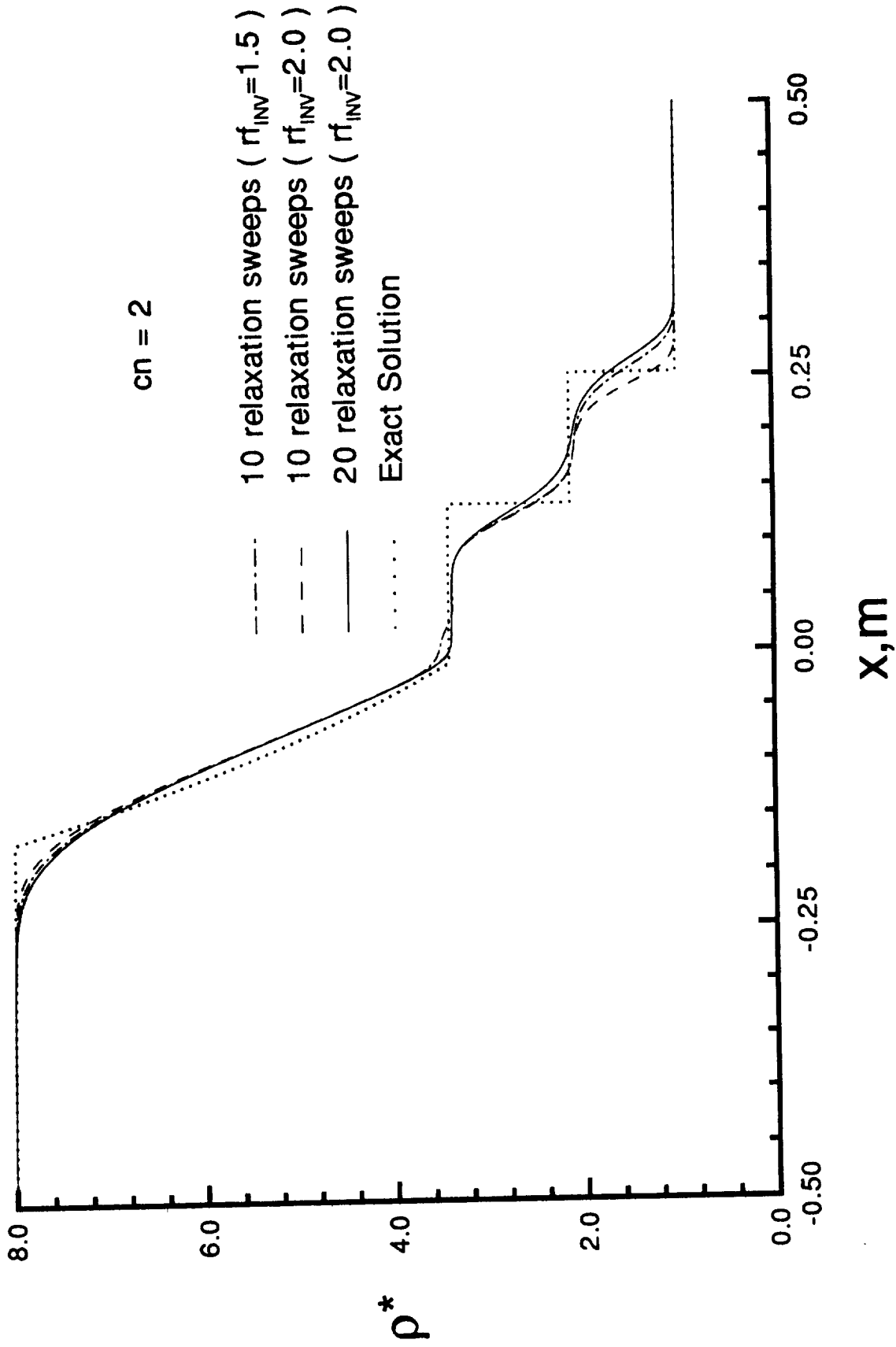


Figure 9. Effect of the inviscid relaxation factor on the nondimensional density distribution for $cn=2$.

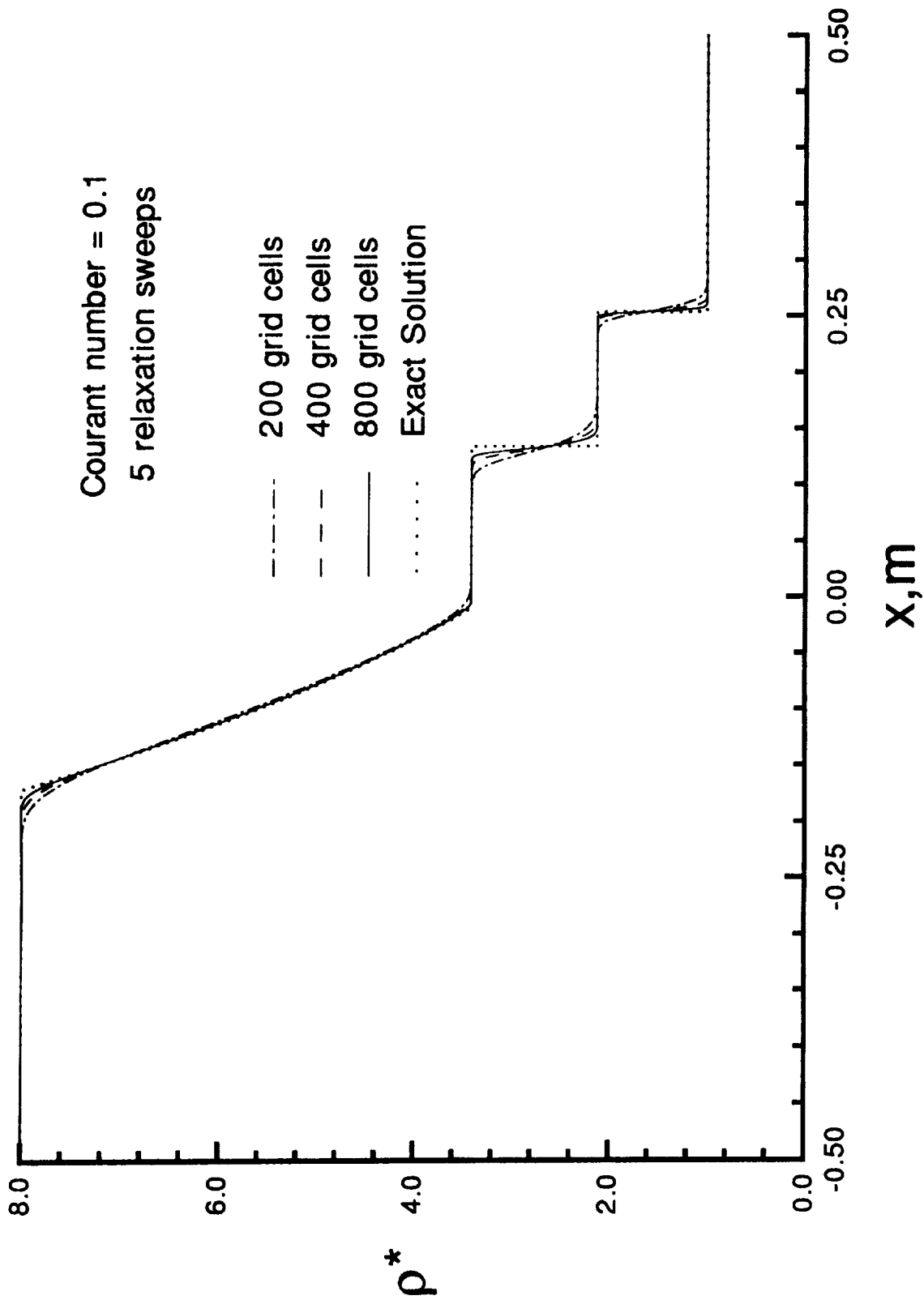


Figure 10. Effect of grid cell spacing on the nondimensional density distribution.

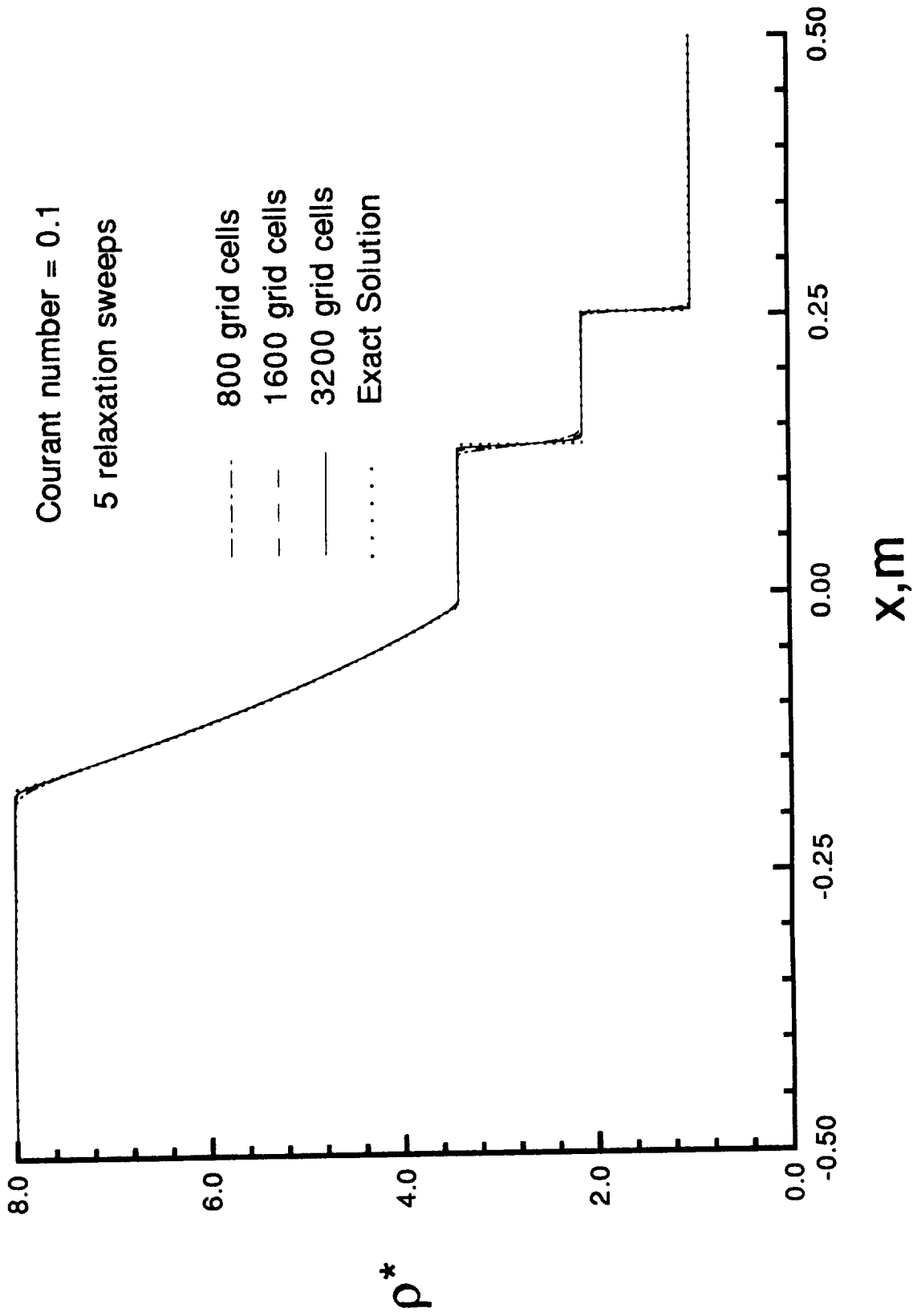


Figure 11. Effect of grid cell spacing on the nondimensional density distribution.

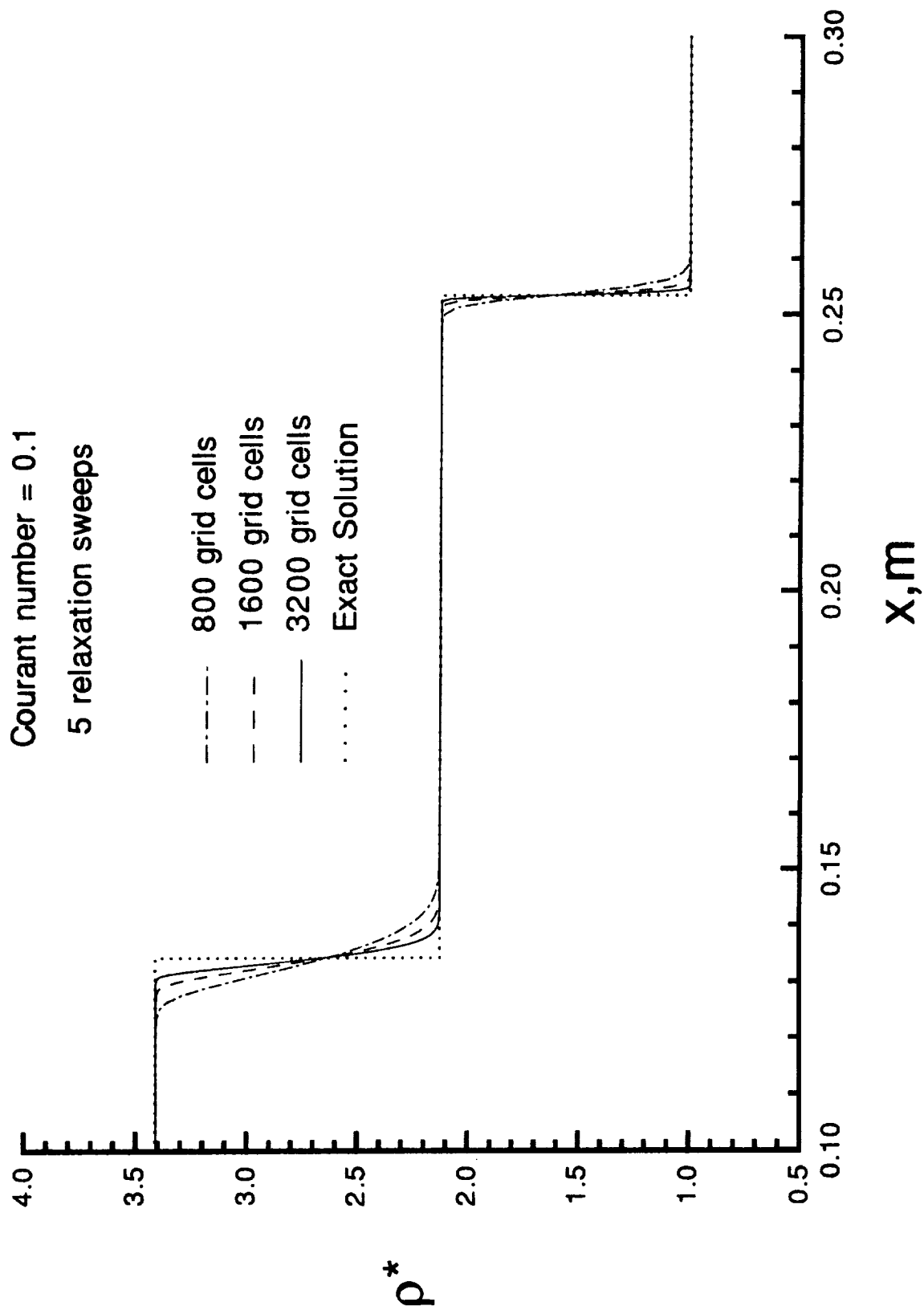


Figure 12. Effect of grid cell spacing on the nondimensional density distribution across the shock and contact surface.

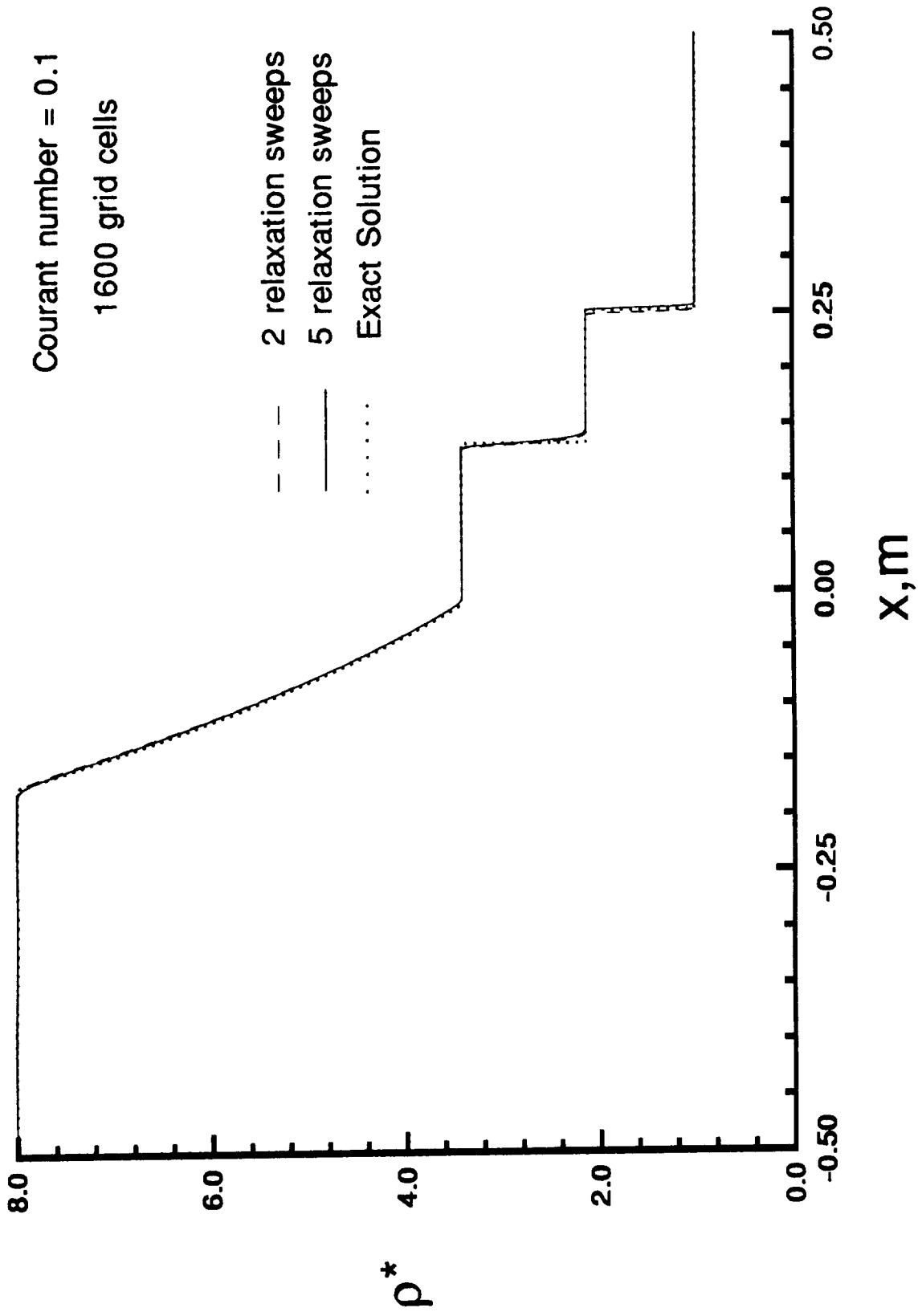


Figure 13. Effect of relaxation sweeps on the nondimensional density distribution.

REPORT DOCUMENTATION PAGE

Form Approved
OMB No. 0704-0188

Public reporting burden for this collection of information is estimated to average 1 hour per response, including the time for reviewing instructions, searching existing data sources, gathering and maintaining the data needed, and completing and reviewing the collection of information. Send comments regarding this burden estimate or any other aspect of this collection of information, including suggestions for reducing this burden, to Washington Headquarters Services, Directorate for Information Operations and Reports, 1215 Jefferson Davis Highway, Suite 1204, Arlington, VA 22202-4302, and to the Office of Management and Budget, Paperwork Reduction Project (0704-0188), Washington, DC 20503.

1. AGENCY USE ONLY (Leave blank)		2. REPORT DATE January 1992	3. REPORT TYPE AND DATES COVERED Technical Memorandum	
4. TITLE AND SUBTITLE Application of Program LAURA to Perfect Gas Shock Tube Flows -- A Parametric Study			5. FUNDING NUMBERS WU 506-40-91-02	
6. AUTHOR(S) K. F. Mitterer, R. A. Mitcheltree, and P. A. Gnoffo				
7. PERFORMING ORGANIZATION NAME(S) AND ADDRESS(ES) NASA Langley Research Center Hampton, VA 23665-5225			8. PERFORMING ORGANIZATION REPORT NUMBER	
9. SPONSORING/MONITORING AGENCY NAME(S) AND ADDRESS(ES) National Aeronautics and Space Administration Washington, DC 20546-0001			10. SPONSORING/MONITORING AGENCY REPORT NUMBER NASA TM-104190	
11. SUPPLEMENTARY NOTES K. F. Mitterer: Langley Research Center, R. A. Mitcheltree: Langley Research Center, and P. A. Gnoffo: Langley Research Center				
12a. DISTRIBUTION/AVAILABILITY STATEMENT Unclassified - Unlimited Subject Category 34			12b. DISTRIBUTION CODE	
13. ABSTRACT (Maximum 200 words) The Langley Aerothermodynamic Upwind Relaxation Algorithm (LAURA) was originally developed to solve steady-flow problems. The desire to validate the algorithm with shock tube experimental data has motivated the development of a time-accurate version of the LAURA code. The current work presents a test of the algorithm. Computational results are compared with the exact solution for a simple shock tube case. The parameters examined are Courant number, relaxation sweeps, grid spacing, and the inviscid relaxation factor. The results of the study indicate that LAURA is capable of producing accurate solutions when appropriate values are used for each parameter.				
14. SUBJECT TERMS Shock tube, Total Variation Diminishing, Perfect Gas, Roe's Averaging, and Computational Analysis			15. NUMBER OF PAGES 22	
			16. PRICE CODE A03	
17. SECURITY CLASSIFICATION OF REPORT Unclassified	18. SECURITY CLASSIFICATION OF THIS PAGE Unclassified	19. SECURITY CLASSIFICATION OF ABSTRACT	20. LIMITATION OF ABSTRACT	



